frontiers in Marine Science

ORIGINAL RESEARCH
published: 15 May 2018
doi: 10.3389/fmars.2018.00167

Aggregate Formation During the Viral Lysis of a Marine Diatom

Yosuke Yamada[1*†], *Yuji Tomaru*[2], *Hideki Fukuda*[1] *and Toshi Nagata*[1]

[1] *Atmosphere and Ocean Research Institute, The University of Tokyo, Chiba, Japan,* [2] *National Research Institute of Fisheries and Environment of Inland Sea, Japan Fisheries Research and Education Agency, Hiroshima, Japan*

Recent studies have suggested that the viral lysis of microbes not only facilitates the conversion of particulate organic matter into dissolved organic matter, but also promotes the formation of organic aggregates, which enhance the export of organic carbon from the surface ocean to the deep sea. However, experimental data supporting this proposition are limited. Here, we tested the hypothesis that the viral infection of marine diatoms enhances aggregate formation. We used a model system consisting of *Chaetoceros tenuissimus,* a bloom-forming diatom with an approximate cell size of 3–10 μm, and a DNA virus, CtenDNAV type II, which replicates in the nucleus of *C. tenuissimus*. The volume of large particles (50–400 μm in equivalent spherical diameters, determined from photographic images) was measured over time (up to 15 days) in the diatom-alone control and a virus-added diatom culture. We also determined the concentrations of Coomassie-stainable particles (CSP, proteinaceous particles) and transparent exopolymeric particles (TEP, acid-polysaccharide-rich particles) with colorimetric methods. The total volume of large particles was significantly higher (5–59 fold) in the virus-added diatoms than in the diatom-alone control during the period in which the viral lysis of the diatoms proceeded. One class of large particles produced in the virus-added diatoms was flake-shaped. The flakes were tightly packed and dense, and sank rapidly, possibly playing an important role in the vertical delivery of materials from the surface to the deep sea. The bulk CSP concentrations tended to be higher in the virus-added diatoms than in the diatom-alone control, whereas the reverse was true for the TEP. These results suggest that proteinaceous polymers are involved in aggregate formation. Our data support the emerging notion that the viral lysis of microbes facilitates aggregate formation and the export of organic carbon in the ocean.

Keywords: aggregate, diatom–virus interaction, particle size distribution, settling velocity, material cycle

OPEN ACCESS

Edited by:
Eric 'Pieter Achterberg, GEOMAR Helmholtz-Zentrum für Ozeanforschung Kiel, Germany

Reviewed by:
Cátia Carreira, University of Aveiro, Portugal
Zrinka Ljubesic, University of Zagreb, Croatia

****Correspondence:***
Yosuke Yamada
yoyamada@ucsd.edu

†Present Address:
Yosuke Yamada, Scripps Institution of Oceanography, University of California, San Diego, San Diego, CA, United States

Specialty section:
This article was submitted to Marine Biogeochemistry, a section of the journal Frontiers in Marine Science

Received: *29 November 2017*
Accepted: *25 April 2018*
Published: *15 May 2018*

Citation:
Yamada Y, Tomaru Y, Fukuda H and Nagata T (2018) Aggregate Formation During the Viral Lysis of a Marine Diatom. Front. Mar. Sci. 5:167. doi: 10.3389/fmars.2018.00167

INTRODUCTION

Viruses are important agents of microbial mortality and may affect biogeochemical cycles in marine environments by promoting the production of dissolved organic matter and enhancing nutrient cycling (viral shunt; Wilhelm and Suttle, 1999; Weinbauer, 2004; Motegi et al., 2009). Viruses may also enhance aggregate formation (Weinbauer, 2004; Sullivan et al., 2017). This hypothesis was first supported by an early study that showed that the abundance of large aggregates in seawater enriched with viruses was higher than that in seawater without viral enrichment (Peduzzi and Weinbauer, 1993). The enhanced aggregate formation was attributed to lysis products and cell residues that

acted as glue, causing the particles to stick together (Peduzzi and Weinbauer, 1993; Weinbauer, 2004; Uitz et al., 2010). More recently, an analysis of environmental and metagenomic data collected in oceans suggested that viruses are a strong predictor of carbon export (the sinking flux of particulate organic carbon) (Guidi et al., 2016). In the North Atlantic, investigators suggested that aggregate formation and vertical carbon fluxes were enhanced by the Coccolithovirus infections of coccolithophore, *Emiliania huxleyi*, blooms (Laber et al., 2018). These results have renewed interest in the role of viruses in promoting biological carbon pumps by enhancing aggregate formation (viral shuttle; Sullivan et al., 2017). However, we know little about the relative importance of "viral shunting" and "viral shuttling" in marine carbon cycling, or how these differ with various types of virus–host systems and environmental conditions.

To clarify the role of viral infection in the regulation of organic carbon export in oceans, we examined whether the viral infection of diatoms enhances aggregate formation. Diatoms are a major oceanic primary producer and contribute greatly to the vertical transport of carbon and other bioelements (Thornton, 2002; Allen et al., 2005; Sarmento et al., 2013). They have silicified cell walls (frustules), which act as high-density ballast, increasing their settling velocity (Ploug et al., 2008; Iversen and Ploug, 2010). Depending on the diatom species and the environmental conditions, diatoms often form aggregates, which are lost from the euphotic zone by settling (Smetacek, 1985). The settling velocities of diatom aggregates can exceed the settling velocities of individual cells or cell chains by as much as an order of magnitude (Passow, 2002). Therefore, diatom aggregation can substantially enhance organic carbon export. Extracellular polymeric substances (EPS; Decho and Gutierrez, 2017) play an important role in the regulation of diatom aggregate formation by enhancing diatom stickiness and coagulation (Kiorboe and Hansen, 1993; Thornton, 2002). Factors that may influence EPS production by diatoms include nutrient conditions and diatom–bacteria interactions (Kiorboe and Hansen, 1993; Gärdes et al., 2012). Viral infection may also affect the host physiology and enhance EPS production by microalgae. In fact, the viral-induced enhancement of transparent exopolymer particle (TEP) production has been observed for *Micromonas pusilla* (Prasinophyceae) (Lønborg et al., 2013), and *E. huxleyi* (Haptophyceae) (Laber et al., 2018). However, whether viral infection affects EPS production and aggregate formation by diatoms has yet to be examined.

We used a model system consisting of *Chaetoceros tenuissimus,* a bloom-forming diatom, and a single-stranded DNA virus, *C. tenuissimus* DNA virus (CtenDNAV type II), which replicates in the nucleus of *C. tenuissimus* (Kimura and Tomaru, 2015). To examine whether the viral infection of diatoms enhances aggregate formation, we measured the abundance and volume of large particles (equivalent spherical diameters [ESD] of 50–400 μm) and their visible morphological category (flakes) in images taken by camera. We also determined the concentrations of two kinds of EPS, TEP (Passow, 2002) and Coomassie-stainable particles (CSP; Long and Azam, 1996), with colorimetric methods.

MATERIALS AND METHODS

Incubation of Diatoms and Viruses

Chaetoceros tenuissimus strain 2–10 (NIES-3715) (Shirai et al., 2008) and CtenDNAV type II, isolated from the coast of western Japan (Kimura and Tomaru, 2015), were used in this study. The cultures were prepared in the laboratory of the National Research Institute of Fisheries and Environment of Inland Seas, Japan, where CtenDNAV type II is maintained by its successive transfer to fresh axenic diatom cultures, as described by Kimura and Tomaru (2015). After staining with 4′,6-diamidino-2-phenylindole (Porter and Feig, 1980), an epifluorescence microscopic analysis revealed that the culture was bacteria-free. CtenDNAV type II could not be counted with epifluorescence microscopy, presumably because their nucleic acid content is low (difficulty in detecting viruses with epifluorescence microscopy or flow cytometry has been reported for other viruses with low nucleic acid contents; Brussaard et al., 2000; Tomaru and Nagasaki, 2007). *Chaetoceros tenuissimus* was incubated in eight replicate glass bottles filled with 1 L of culture medium. The culture medium was composed of 0.25 g of Daigo IMK medium (Nihon Pharmaceutical Co., Ltd, Tokyo, Japan) and 56.8 mg of $Na_2SiO_3 \cdot 9H_2O$ dissolved in 1 L of 0.2 μm-filtered coastal seawater (salinity, 33.1). Before the inoculation of the culture medium with *C. tenuissimus*, it was autoclaved (15 min, 120°C) and then filtered through a 0.2 μm filter to remove any particles produced during the preparation of the medium. The cultures were incubated at 20°C in an illuminated incubator (12/12 h light/dark cycle with 150 μmol photons m^{-2} s^{-1}) under static conditions. After incubation for 6 days, 1 mL of CtenDNAV stock (5.1×10^9 infectious units mL^{-1}) was added to each of four replicate *C. tenuissimus* cultures (virus-added diatoms). A CtenDNAV type II stock that had been autoclaved was added to the remaining four replicate cultures (diatom-alone controls). Subsamples were withdrawn from the cultures at intervals of either 1 day (300 μL each, for the measurement of diatom cell abundance) or 3 days (100 mL each, for the measurement of particle abundance, size, and volume; and 10 mL each, for the measurement of TEP and CSP concentrations). The handling time required for each round of subsampling was < 1 h.

Diatom abundance was determined with a Thoma cell counting chamber under a light microscope (BX-61; Olympus, Tokyo, Japan). Only intact cells with clear cell walls were counted. Cells in at least 32 discrete fields were counted on each slide.

Particle Size, Volume, and Abundance

The size, volume, and abundance of the large particles were analyzed with an image analysis, from images captured with a camera, according to Yamada et al. (2013). Subsamples were placed in 70 mL glass rolling tubes and laterally illuminated with a flashlight, and the images were taken with a digital camera (EOS Kiss X6i; Canon, Tokyo, Japan) (**Figure 1A**). The images obtained were analyzed with the ImageJ software (v.1.45 with Java, 1.6.0_20). Large particles were defined to be the objects with areas exceeding 2.0×10^{-5} cm^2 (33 pixels) (**Figure 1B**). One class of large particles, flake-shaped particles (flat or thinly rolled films with polyangular [mostly

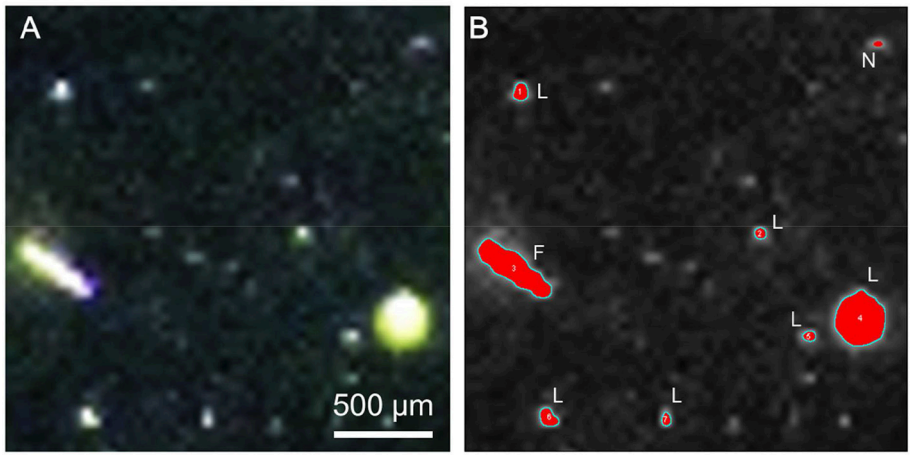

FIGURE 1 | Large particles produced in virus-added diatom culture. **(A)** Photographic image. **(B)** Extracted objects (red) after image processing with the ImageJ software. L: large particle; F: flake; N: not examined because the area was $< 2.0 \times 10^{-5}$ cm^2 (see Materials and Methods).

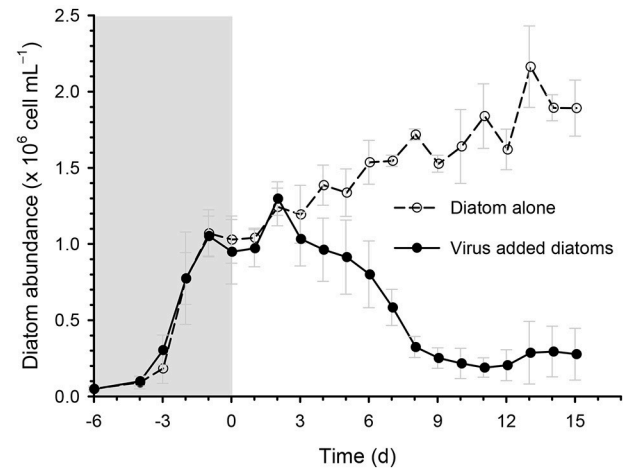

FIGURE 2 | Time course of the changes in diatom abundance during incubation in the diatom-alone control and virus-added diatoms. Viruses were inoculated on day 0. Values are means ± standard deviation (SD, $n = 4$).

quadrangular] shapes), with an approximate linear dimension of 100–1,000 μm, were conspicuous in the virus-added diatoms (see Results and Discussion), and we determined the abundance and volume of these flakes separately (**Figure 1B**).

Characterization of Flake-Shaped Particles

We examined whether the flakes were stainable with Alcian Blue 8GX (Sigma-Aldrich, St. Louis, MO, USA) and Coomassie Brilliant Blue G-250 (CBB; Serva Electrophoresis GmbH, Heidelberg, Germany) using samples collected on day 15. The flakes were stained with either 0.02% (w/v) Alcian Blue dissolved in 0.06% (v/v) acetic acid or 0.04% CBB (pH 7.4) and observed under a light microscope (BX-61; Olympus).

The size distribution and settling velocities of the flakes were examined using the flakes collected on day 18. The flakes were placed in a petri dish and their images were captured with a digital camera to determine their ESD distribution. The settling velocity of the flakes was determined with the sedimentation column method (Ploug et al., 2010; Yamada et al., 2016). A 1 L graduated cylinder (7 cm wide) was filled with 0.2 μm filtered seawater (salinity, 23.6) and stabilized in a temperature-controlled room (23.5°C). For each round of measurement, a flake was gently introduced into the upper part of the water column with a micropipette and its travel time over a distance of 20.5 cm was recorded with a stopwatch. In total, we examined the settling velocities of 32 flakes to cover a range of ESD. The settling velocities (U, m d^{-1}) of the flakes were related to ESD (d, m) using the power regression. From the exponent (ε) of the power regression, the fractal dimension (D_f) of the flakes was estimated: $D_f = \varepsilon + 1$ (Logan and Wilkinson, 1990). We then calculated the density of the flakes (ρ_s, g cm^{-3}) using the Stokes model (Heiss and Coull, 1952):

$$\rho_s = \rho_f + \frac{18\,\mu\,U}{K\,g\,d^2}, \quad (1)$$

where g is the gravitational acceleration (m s^{-2}), ρ_f is the density of seawater (g cm^{-3}), μ is the viscosity of seawater (kg m^{-1} s^{-1}), and K is a dimensionless shape-correction factor. The calculation was performed with the density (1.015 g cm^{-3}) and viscosity (0.00098 kg m^{-1} s^{-1}) of seawater at 23.5°C, with a salinity of 23.6 (Fofonoff and Millard, 1983), and on the assumption that the settling velocity of the flake-shaped particles was 0.4–0.6 times lower than that of spherical particles (i.e., $K = 0.4$–0.6 for disc-shaped particles; Heiss and Coull, 1952; Happel and Brenner, 1983).

CSP and TEP Concentrations

The concentrations of particles containing proteins (CSP) and acid-polysaccharides (TEP) were measured according to Cisternas-Novoa et al. (2014) and Passow and Alldredge (1995), respectively. Because we used colorimetric methods

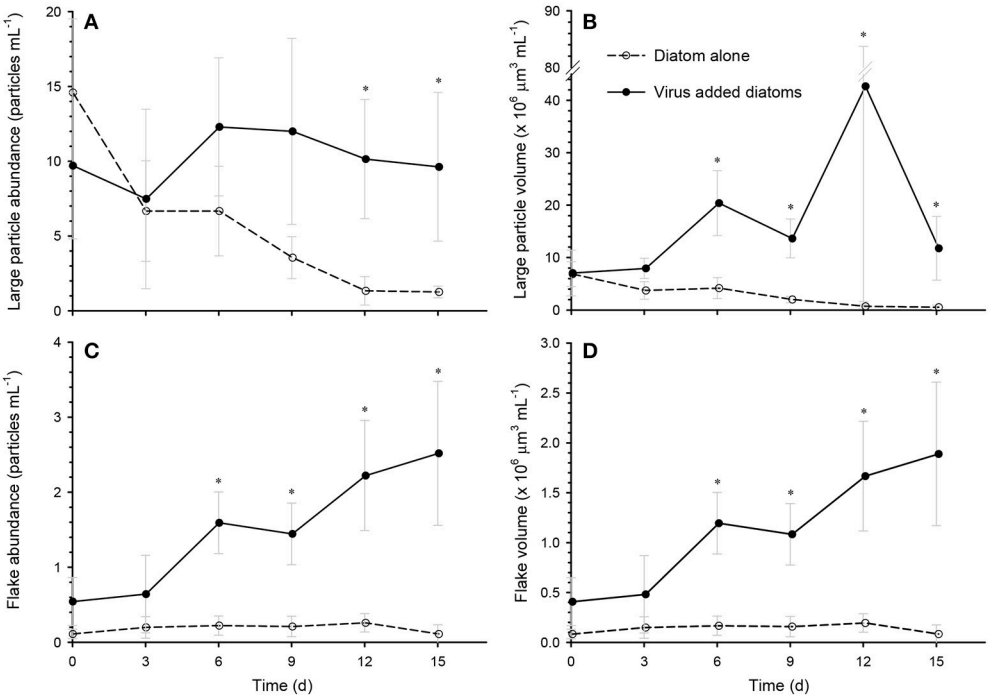

FIGURE 3 | Time course of the changes in the particle abundances and volumes of **(A,B)** large particles, and **(C,D)** flakes in the diatom-alone control and the virus-added diatoms. Asterisks indicate that the differences between the diatom-alone control and the virus-added diatoms were significant ($p < 0.05$; Mann-Whitney-Wilcoxon test). Values are means ± SD ($n = 4$). At each time point, the total number of large particles examined was 17–197 for the diatom-alone control and 57–133 for the virus-added diatoms. The corresponding value for flakes was 1–7 for the diatom-alone control and 11–52 for the virus-added diatoms.

and bulk (non-size-fractionated) samples, we lack information on the size distributions of these particles. Subsamples were filtered through 0.4 µm-pore-sized polycarbonate filters (25 mm diameter; *Whatman*) under a vacuum of < 150 mmHg. For CSP, the filters were stained with 0.04% CBB at pH 7.4. The filters were soaked in 3% sodium dodecyl sulfate in 50% isopropyl alcohol and sonicated in a glass vial for 2 h at 37°C. The absorbance at 615 nm was measured with a spectrophotometer (UV-1800; Shimadzu, Kyoto, Japan). For TEP, the filters were stained with 0.02% (w/v) Alcian Blue 8GX dissolved in 0.06% (v/v) acetic acid. The filters were soaked in 80% sulfuric acid for 3 h and the absorbance at 787 nm was measured spectrophotometrically. The CSP and TEP concentrations were calculated with calibration factors determined with bovine serum albumin (BSA) and xanthan gum, respectively, and expressed as µg BSA equivalents per liter (µg BSAeq. L^{-1}) and µg xanthan gum equivalents per liter (µg Xeq. L^{-1}), respectively.

Statistical Analysis

We used the Mann-Whitney-Wilcoxon test to compare the mean values of particle and EPS parameters between the diatom-alone controls and the virus-added diatom cultures. The exponent of the power regression that related the settling velocity to ESD was estimated by a non-linear curve fitting using SigmaPlot 13.0 (Systat Software).

RESULTS AND DISCUSSION

Dynamics of Diatoms and Large Particles

The addition of the virus CtenDNAV type II to a culture of the diatom *C. tenuissimus* caused a sharp decline (by approximately 10-fold) in diatom abundance after day 3 (**Figure 2**). This decline was accompanied by the clearing of the culture, which indicated algal cell lysis (Kimura and Tomaru, 2015). A similar time course of *C. tenuissimus* abundance after inoculation with CtenDNAV type II has been described previously (Kimura and Tomaru, 2015).

The abundance and volume of the large particles decreased over time in the diatom-alone control, reaching the lowest levels (1.3 particles mL^{-1} and 0.5 × 10^6 µm^3 mL^{-1}, respectively) on day 15 (**Figures 3A,B**). In contrast, the large particle abundance remained high (7–12 particles mL^{-1}) in the virus-added diatoms during the whole incubation period, and was significantly higher than that in the diatom-alone control on day 12 and day 15 (**Figure 3A**). The total volume of large particles was significantly larger (5–59 fold) than in the diatom-alone control on days 6, 9, 12, and 15 (**Figure 3B**). Although the errors associated with the estimates of the total volume of particles were large especially on day 12, our statistical results using the non-parametric test indicated that the differences in the total volume between the virus-added diatoms and the diatom-alone control were significant ($p < 0.05$). For the virus-added diatoms, our results also showed that the total volume of large particles on

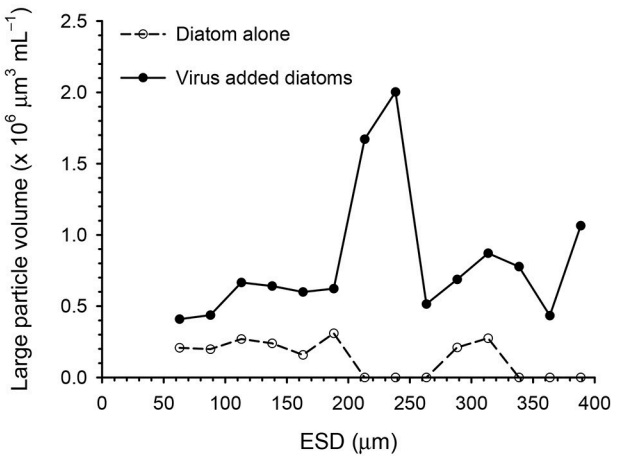

FIGURE 4 | Size distributions of large particles in the diatom-alone control and the virus-added diatoms. The data obtained on days 6, 9, 12, and 15 were pooled. Total number of particles determined was 173 for the diatom-alone control and 405 for the virus-added diatoms.

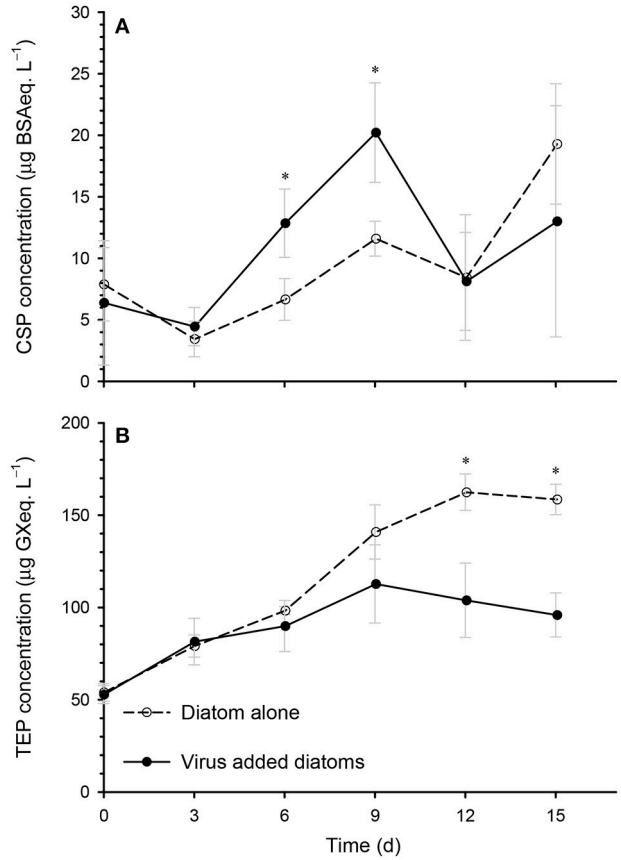

FIGURE 5 | Time course of the changes in the concentrations of **(A)** Coomassie-stainable particles (CSP), and **(B)** transparent exopolymer particles (TEP) in the diatom-alone control and the virus-added diatoms. Asterisks indicate that the differences between the diatom-alone control and the virus-added diatoms were significant ($p < 0.05$; Mann-Whitney-Wilcoxon test). Values are means ± SD ($n = 4$).

days 6, 9, 12, and 15 (during the viral lysis of diatoms) were significantly ($p < 0.05$; Mann-Whitney-Wilcoxon test) larger than that on day 0 (before the viral lysis). The higher total volume of large particles during the viral lysis (**Figure 3B**), with no concomitant increase in particle abundance during the same period (**Figure 3A**), might indicate that smaller particles, which were below the detection limit of our image analysis, stuck to large particles to lead to the increase in the volume of individual large particles (i.e., the scavenging of small particles by large particles; Jackson and Burd, 2015), although this proposition must be verified by future studies. These results indicate that the formation of aggregates (large particles) was enhanced by the viral lysis of diatoms. When the data collected on days 6, 9, 12, and 15 were pooled, the size distribution of the large particles in the virus-added diatoms peaked at approximately at 240 μm, whereas that in the diatom-alone control showed no clear peak (**Figure 4**).

Occurrence and Characterization of Flake-Shaped Aggregates

One class of large particles produced in the virus-added diatoms was flake-shaped particles. Both the abundance and total volume of the flakes increased after day 6 and they reached their maximum abundance (2.5 particles mL^{-1}) and volume (2.0×10^6 μm^3 mL^{-1}) on day 15 (**Figures 3C,D**), when the flakes accounted for 17% of the large particle volume in the virus-added diatoms. In contrast, negligible flakes were observed ($< 0.21 \times 10^6$ μm^3 mL^{-1} or < 0.27 particles mL^{-1}) in the diatom-alone control. The flakes were stained by Alcian Blue and CBB (Supplementary Figure S1), indicating that they contained acidic polysaccharides and proteins. Under the condition of our microscopic observations, frustule fragments of diatoms (or frustule-like structures) were not associated with the flakes. The settling velocities of the flakes (89–142 μm, ESD) varied in the range of 35–113 m $days^{-1}$. From the relationship between the settling velocity and the size of the flakes (Supplementary Figure S2), the fractal dimension of the flakes was estimated to be 3.09 ± 0.27. The fractal dimension describes a geometric feature (spatial structure) of the aggregates and a high value (close to 3) generally indicates that the aggregates are tightly packed (Logan and Wilkinson, 1990). The density of the flakes was estimated to be 1.26–1.39 g cm^{-3}. This density is lower than that of silicified cell-wall fragments (2.09 g cm^{-3}; Ploug et al., 2010; Deer et al., 2013), but corresponds to the upper range of densities previously reported for marine aggregates (1.08–1.35 g cm^{-3}; Alldredge and Gotschalk, 1988; Ploug et al., 2008; Lombard et al., 2013). Taken together, the histochemical (stainable with Alcian Blue and CBB), geometric (high fractal dimension), and physical properties (high density) of the flakes suggest that they are probably highly packed aggregates containing dense constituents bound by polysaccharides and proteins. Although flake-shaped particles (also described as "films" or "sheets" in the literature) have previously been observed in marine environments (Johannes, 1967; Gordon, 1970; Emery et al., 1984; Alldredge et al., 1993), it

is unclear whether they correspond to the flakes that we found in the virus-added diatom cultures. Given the high settling velocity of the flakes in the virus-added diatom cultures, these particles may play an important role in the vertical transport of carbon and other bioelements from the ocean surface to the deeper ocean. The flakes might also act as high-density ballast if they are incorporated into larger aggregates by coagulation.

Effects of Viral Infection on EPS Dynamics

Extracellular polymeric particles containing CSP (protein-rich particles) and TEP (acid-polysaccharide-rich particles) may act as a glue to promote the coagulation of particles, and may therefore be involved in the formation of diatom aggregates (Long and Azam, 1996; Passow, 2002; Mari et al., 2017). Our data show that the CSP concentration in the virus-added diatoms was significantly higher than that in the diatom-alone control on days 6 and 9 (**Figure 5A**), which corresponded to the increase in the volume of large particles (**Figure 3**). This may indicate that aggregate formation was enhanced by proteinaceous particles. In contrast, we found that the TEP concentration in the virus-added diatoms tended to be lower than the corresponding concentration in the diatom-alone control (**Figure 5B**). This contradicts previous findings in *M. pusilla* (Lønborg et al., 2013) and *E. huxleyi* (Laber et al., 2018) that TEP production was enhanced by viral infection. These results indicate that the effects of viral infection on TEP production by marine microalgae depend on the species of alga, the virus, or both. Further studies are required to investigate the role of TEP in aggregate (including flakes) formation in the virus-added diatom cultures and the physiological mechanisms by which CSP and TEP production is regulated in alga–virus systems.

CONCLUSIONS AND FUTURE PERSPECTIVES

Our data showed that large aggregates, including flakes, were produced during viral lysis of diatoms. The flakes were dense and closely packed, and sank rapidly, suggesting that they play an important role in the vertical delivery of organic carbon in the ocean. Proteinaceous polymeric particles (CSP) probably facilitate aggregate formation, although more data are required on the role of TEP and other particles in the regulation of aggregate dynamics. We stress that our results from pure laboratory cultures, using *C. tenuissimus* and CtenDNAV as a model diatom–virus system, may not be simply applicable to natural environments. The aggregate-forming characteristics of diatoms vary among diatom species and even within the same species, depending on the growth conditions (Kiorboe and Hansen, 1993; Thornton, 2002; Laurenceau-Cornec et al., 2015). Further studies are required to examine whether the extent and nature of virally induced increases in aggregate formation differ across different types of diatom–virus systems. Although we focused on a diatom–virus system in this study, various microbes are present in real oceans, including bacteria and protist grazers, which may also substantially affect aggregate formation and disintegration through their metabolic activities (Azam and Malfatti, 2007; Jackson and Burd, 2015; Yamada et al., 2016) as does the viral lysis of these cells (Weinbauer, 2004; Sullivan et al., 2017).

Despite the limitations of this study, our data support the emerging concept of the "viral shuttle" (Weinbauer, 2004; Sullivan et al., 2017), which suggests that the conventional model of virus-driven biogeochemical cycles ("viral shunt") should be revised to include the aggregation pathway by which lysed algal material is subject to sinking loss. A comprehensive understanding of the role of viral infection in regulating the biological carbon pump should improve our ability to predict the future states of ocean biogeochemical cycles.

AUTHOR CONTRIBUTIONS

YY, YT, and TN designed the experiment; YY and YT cultured the diatoms and viruses, and YY conducted the particle and flake analyses; YY, YT, HF, and TN analyzed the data and wrote the paper.

FUNDING

This study was supported by the Japan Society for the Promotion of Science (JSPS) KAKENHI, grant numbers 15H01725 and 17H06294 awarded to TN and grant number 16H06429, 16K21723, and 16H06437 awarded to YT.

ACKNOWLEDGMENTS

We thank Markus Weinbauer for his valuable comments on the early version of this manuscript.

SUPPLEMENTARY MATERIAL

The Supplementary Material for this article can be found online at: https://www.frontiersin.org/articles/10.3389/fmars.2018.00167/full#supplementary-material

REFERENCES

Alldredge, A., and Gotschalk, C. (1988). *In situ* settling behavior of marine snow. *Limnol. Oceanogr.* 33, 339–351. doi: 10.4319/lo.1988.33.3.0339

Alldredge, A., Passow, U., and Logan, B. E. (1993). The abundance and significance of a class of large, transparent organic particles in the ocean. *Deep Sea Res. I* 40, 1131–1140. doi: 10.1016/0967-0637(93)90129-Q

Allen, J. T., Brown, L., Sanders, R., Moore, C. M., Mustard, A., Fielding, S., et al. (2005). Diatom carbon export enhanced by silicate upwelling in the northeast Atlantic. *Nature* 437, 728–732. doi: 10.1038/nature03948

Azam, F., and Malfatti, F. (2007). Microbial structuring of marine ecosystems. *Nat. Rev. Microbiol.* 5, 782–791. doi: 10.1038/nrmicro1747

Brussaard, C. P., Marie, D., and Bratbak, G. (2000). Flow cytometric detection of viruses. *J. Virol. Methods* 85, 175–182. doi: 10.1016/S0166-0934(99)00167-6

Cisternas-Novoa, C., Lee, C., and Engel, A. (2014). A semi-quantitative spectrophotometric, dye-binding assay for determination of Coomassie Blue stainable particles. *Limnol. Oceanogr. Meth.* 12, 604–616. doi: 10.4319/lom.2014.12.604

Decho, A. W., and Gutierrez, T. (2017). Microbial extracellular polymeric substances (EPSs) in ocean systems. *Front. Microbiol.* 8:922. doi: 10.3389/fmicb.2017.00922

Deer, W. A., Howie, R. A., and Zussman, J. (2013). *An Introduction to the Rock-Forming Minerals, 3rd Edn*. London: The Mineralogical Society.

Emery, K. O., Johns, I. A., and Honjo, S. (1984). Organic films on particulate matter in surface waters off eastern Asia. *Sedimentology* 31, 503–514. doi: 10.1111/j.1365-3091.1984.tb01816.x

Fofonoff, N., and Millard, R. J. (1983). *Algorithms for Computation of Fundamental Properties of Seawater*. "UneSCO" Technical Papers in Marine Science.

Gärdes, A., Ramaye, Y., Grossart, H. P., Passow, U., and Ullrich, M. S. (2012). Effects of *Marinobacter adhaerens* HP15 on polymer exudation by *Thalassiosira weissflogii* at different N:P ratios. *Mar. Ecol. Prog. Ser.* 461, 1–14. doi: 10.3354/meps09894

Gordon, D. C. (1970). A microscopic study of organic particles in the North Atlantic Ocean. *Deep Sea Res.* 17, 175–185. doi: 10.1016/0011-7471(70)90096-3

Guidi, L., Chaffron, S., Bittner, L., Eveillard, D., Larhlimi, A., Roux, S., et al. (2016). Plankton networks driving carbon export in the oligotrophic ocean. *Nature* 532, 465–470. doi: 10.1038/nature16942

Happel, J., and Brenner, H. (1983). *Low Reynolds Number Hydrodynamics With Special Applications to Particulate Media*. Dordrecht: Kluwer Academic.

Heiss, J., and Coull, J. (1952). The effect of orientation and shape on the settling velocity of non-isometric particles in a viscous medium. *Chem. Eng. Progr.* 48, 133–140.

Iversen, M. H., and Ploug, H. (2010). Ballast minerals and the sinking carbon flux in the ocean: carbon-specific respiration rates and sinking velocity of marine snow aggregates. *Biogeosciences* 7, 2613–2624. doi: 10.5194/bg-7-2613-2010

Jackson, G. A., and Burd, A. B. (2015). Simulating aggregate dynamics in ocean biogeochemical models. *Prog. Oceanogr.* 133, 55–65. doi: 10.1016/j.pocean.2014.08.014

Johannes, R. E. (1967). Ecology of organic aggregates in the vicinity of a coral reef. *Limnol. Oceanogr.* 12, 189–195. doi: 10.4319/lo.1967.12.2.0189

Kimura, K., and Tomaru, Y. (2015). Discovery of two novel viruses expands the diversity of single-stranded DNA and single-stranded RNA viruses infecting a cosmopolitan marine diatom. *Appl. Environ. Microbiol.* 81, 1120–1131. doi: 10.1128/AEM.02380-14

Kiorboe, T., and Hansen, J. L. S. (1993). Phytoplankton aggregate formation—observations of patterns and mechanisms of cell sticking and the significance of exopolymeric material. *J. Plankton Res.* 15, 993–1018. doi: 10.1093/plankt/15.9.993

Laber, C. P., Hunter, J. E., Carvalho, F., Collins, J. R., Hunter, E. J., Schieler, B. M., et al. (2018). Coccolithovirus facilitation of carbon export in the North Atlantic. *Nat. Microbiol.* 3, 537–547. doi: 10.1038/s41564-018-0128-4

Laurenceau-Cornec, E. C., Trull, T. W., Davies, D. M., De La Rocha, C. L., and Blain, S. (2015). Phytoplankton morphology controls on marine snow sinking velocity. *Mar. Ecol. Prog. Ser.* 520, 35–56. doi: 10.3354/meps11116

Logan, B. E., and Wilkinson, D. B. (1990). Fractal geometry of marine snow and other biological aggregates. *Limnol. Oceanogr.* 35, 130–136. doi: 10.4319/lo.1990.35.1.0130

Lombard, F., Guidi, L., and Kiorboe, T. (2013). Effect of type and concentration of ballasting particles on sinking rate of marine snow produced by the appendicularian *Oikopleura dioica*. *PLoS ONE* 8:e75676. doi: 10.1371/journal.pone.0075676

Lønborg, C., Middelboe, M., and Brussaard, C. (2013). Viral lysis of *Micromonas pusilla*: impacts on dissolved organic matter production and composition. *Biogeochemistry* 116, 231–240. doi: 10.1007/s10533-013-9853-1

Long, R. A., and Azam, F. (1996). Abundant protein-containing particles in the sea. *Aquat. Microb. Ecol.* 10, 213–221. doi: 10.3354/ame010213

Mari, X., Passow, U., Migon, C., Burd, A. B., and Legendre, L. (2017). Transparent exopolymer particles: effects on carbon cycling in the ocean. *Progr. Oceanogr.* 151, 13–37. doi: 10.1016/j.pocean.2016.11.002

Motegi, C., Nagata, T., Miki, T., Weinbauer, M. G., Legendre, L., and Rassoulzadegan, F. (2009). Viral control of bacterial growth efficiency in marine pelagic environments. *Limnol. Oceanogr.* 54, 1901–1910. doi: 10.4319/lo.2009.54.6.1901

Passow, U. (2002). Transparent exopolymer particles (TEP) in aquatic environments. *Progr. Oceanogr.* 55, 287–333. doi: 10.1016/S0079-6611(02)00138-6

Passow, U., and Alldredge, A. L. (1995). A dye-binding assay for the spectrophotometric measurement of transparent exopolymer particles (TEP). *Limnol. Oceanogr.* 40, 1326–1335. doi: 10.4319/lo.1995.40.7.1326

Peduzzi, P., and Weinbauer, M. (1993). Effect of concentrating the virus-rich 2–200-nm size fraction of seawater on the formation of algal floes (marine snow). *Limnol. Oceanogr.* 38, 1562–1565. doi: 10.4319/lo.1993.38.7.1562

Ploug, H., Iversen, M. H., Koski, M., and Buitenhuis, E. T. (2008). Production, oxygen respiration rates, and sinking velocity of copepod fecal pellets: direct measurements of ballasting by opal and calcite. *Limnol. Oceanogr.* 53, 469–476. doi: 10.4319/lo.2008.53.2.0469

Ploug, H., Terbruggen, A., Kaufmann, A., Wolf-Gladrow, D., and Passow, U. (2010). A novel method to measure particle sinking velocity *in vitro*, and its comparison to three other *in vitro* methods. *Limnol. Oceanogr. Meth.* 8, 386–393. doi: 10.4319/lom.2010.8.386

Porter, K. G., and Feig, Y. S. (1980). The use of DAPI for identifying and counting aquatic microflora. *Limnol. Oceanogr.* 25, 943–948. doi: 10.4319/lo.1980.25.5.0943

Sarmento, H., Romera-Castillo, C., Lindh, M., Pinhassi, J., Sala, M. M., Gasol, J. M., et al. (2013). Phytoplankton species-specific release of dissolved free amino acids and their selective consumption by bacteria. *Limnol. Oceanogr.* 58, 1123–1135. doi: 10.4319/lo.2013.58.3.1123

Shirai, Y., Tomaru, Y., Takao, Y., Suzuki, H., Nagumo, T., and Nagasaki, K. (2008). Isolation and characterization of a single-stranded RNA virus infecting the marine planktonic diatom *Chaetoceros tenuissimus* Meunier. *Appl. Environ. Microbiol.* 74, 4022–4027. doi: 10.1128/AEM.00509-08

Smetacek, V. S. (1985). Role of sinking in diatom life-history cycles: ecological, evolutionary and geological significance. *Mar. Biol.* 84, 239–251. doi: 10.1007/BF00392493

Sullivan, M. B., Weitz, J. S., and Wilhelm, S. W. (2017). Viral ecology comes of age. *Environ. Microbiol. Rep.* 9, 33–35. doi: 10.1111/1758-2229.12504

Thornton, D. C. O. (2002). Diatom aggregation in the sea: mechanisms and ecological implications. *Eur. J. Phycol.* 37, 149–161. doi: 10.1017/S0967026202003657

Tomaru, Y., and Nagasaki, K. (2007). Flow cytometric detection and enumeration of DNA and RNA viruses infecting marine eukaryotic microalgae. *J. Oceanogr.* 63, 215–221. doi: 10.1007/s10872-007-0023-8

Uitz, J., Stramski, D., Baudoux, A.-C., Reynolds, R. A., Wright, V. M., Dubranna, J., et al. (2010). Variations in the optical properties of a particle suspension associated with viral infection of marine bacteria. *Limnol. Oceanogr.* 55, 2317–2330. doi: 10.4319/lo.2010.55.6.2317

Weinbauer, M. G. (2004). Ecology of prokaryotic viruses. *FEMS Microbiol. Rev.* 28, 127–181. doi: 10.1016/j.femsre.2003.08.001

Wilhelm, S. W., and Suttle, C. A. (1999). Viruses and nutrient cycles in the sea—viruses play critical roles in the structure and function of aquatic food webs. *Bioscience* 49, 781–788. doi: 10.2307/1313569

Yamada, Y., Fukuda, H., Inoue, K., Kogure, K., and Nagata, T. (2013). Effects of attached bacteria on organic aggregate settling velocity in seawater. *Aquat. Microb. Ecol.* 70, 261–272. doi: 10.3354/ame01658

Yamada, Y., Fukuda, H., Tada, Y., Kogure, K., and Nagata, T. (2016). Bacterial enhancement of gel particle coagulation in seawater. *Aquat. Microb. Ecol.* 77, 11–22. doi: 10.3354/ame01784

Conflict of Interest Statement: The authors declare that the research was conducted in the absence of any commercial or financial relationships that could be construed as a potential conflict of interest.